Inorganica Chimica Acta, *119* (1986) 67–74

The EPR Spectrum of Mn(II) Doped into *cis*-Diaquobis(1,1,1,5,5,5-hexafluoroacetylacetonato)zinc(II) and *trans*-Diaquobis(1,1,1,5,5,5-hexafluoroacetylacetonato)zinc(II) and the Crystal Structure of the Host Crystals

RICHARD P. ADAMS, HARRY C. ALLEN, Jr.*

Department of Chemistry, Clark University, Worcester, Maine 01610, U.S.A.

URSZULA RYCHLEWSKA** and DEREK J. HODGSON*

Department of Chemistry, University of North Carolina, Chapel Hill, N.C. 27514, U.S.A.

(Received March 13, 1986)

Abstract

The room temperature electron paramagnetic resonance (EPR) spectrum of *cis*-diaquobis(1,1,1,5,5,-hexafluoroacetylacetonato)manganese(II), Mn(hfa)$_2$, and *trans*-diaquobis(1,1,1,5,5,5-hexafluoroacetylacetonato)manganese(II) hydrate, Mn(hfa)$_2$·H$_2$O, doped into a single crystal of the corresponding zinc(II) chelates has been studied. The crystal structures of the two host chelates have been determined by X-ray crystallographic methods. The *trans* complex crystallizes in the orthorhombic space group *Pnma* with 4 molecules in a cell of dimensions $a = 7.430(5)$, $b = 21.965(8)$, $c = 11.096(4)$ Å; the structure has been refined to a final *R*-factor of 0.057 based on 821 independent reflections. The *cis* complex crystallizes in the monoclinic space group *C*2/*c* with 4 molecules in a cell of dimensions $a = 21.339(3)$, $b = 8.228(3)$, $c = 9.761(4)$ Å, $\beta = 95.99(2)°$; the structure has been refined to a final *R*-factor of 0.041 based on 1170 independent intensities. The spin-Hamiltonian parameters have been determined by the use of energy expressions, complete to the second order of approximation, and by fitting the 30-line spectrum along each of the principal magnetic-axes by the method of least squares. The following results were obtained for the usual spin-Hamiltonian parameters. Mn(hfa)$_2$: $g_x = 2.0098 = 0.0003$, $g_y = 1.9999 = 0.0003$, $g_z = 2.0002 = 0.0003$, $A_x = 86.44 \times 10^{-4}$ cm^{-1}, $A_y = 86.52 \times 10^{-4}$ cm^{-1}, $A_z = 86.53 \times 10^{-4}$ cm^{-1}, $D = 158.81 \times 10^{-4}$ cm^{-1}, $E = 8.4 \times 10^{-4}$ cm^{-1}. Mn(hfa)$_2$·H$_2$O: $g_z = 1.9960 = 0.0003$, $A_z = 85.68 \times 10^{-4}$ cm^{-1}, $D = 374.45 \times 10^{-4}$ cm^{-1}, $E = 66.24 \times 10^{-4}$ cm^{-1}. The spectrum of Mn(hfa)$_2$·H$_2$O doped into single crystals of the corresponding magnesium chelate has also been observed. The spin-Hamiltonian parameters are the same, within experimental error, as those for the zinc host lattice.

Introduction

The EPR spectrum arising from manganese(II) has been of considerable interest. The ground state of the free Mn(II) ion is a $^6S_{5/2}$ and is well separated from higher electronic states. If this ground state were preserved in chemical environments, the EPR would be very simple. The sextet would have no splitting except that due to the Zeeman interaction and a single line would be observed at $g = 2.0023$.

The EPR spectrum of Mn(II) has been reported with Mn(II) substituted into a variety of host lattices. Most of the host lattices were those of hydrates or simple ionic salts [1]. Only a few coordination compounds have been investigated in host single crystals [2–5]. In all cases the observed spectrum is very complex, indicating that the environment does exert considerable effect on the ion. In this paper we report the results of the EPR investigation of the isomeric chelates, *cis*- and *trans*-diaquobis(1,1,1,5,5,5-hexafluoroacetylacetonato)manganese(II). These Mn(II) chelates were doped into single crystals of the corresponding zinc(II) chelates, namely, *cis*-diaquobis(1,1,1,5,5,5-hexafluoroacetylacetonato)Zn(II), [Zn(hfa)$_2$] and *trans*-diaquobis(1,1,1,5,5,5-hexafluoroacetylacetonato)Zn(II) hydrate [Zn(hfa)$_2$]·H$_2$O. The structures of the two host Zn(II) chelates have been determined by X-ray methods and are reported here. The *trans*-form was also investigated by using the magnesium chelate as the host. This chelate is presumably isomorphous with the *trans*-zinc chelate.

The spectra are analyzed in terms of a spin-Hamiltonian, and the usual parameters determined. Due to the large deviation from cubic symmetry it

---

*Authors to whom correspondence should be addressed.

**On leave from Department of Chemistry, A. Mickiewicz University, ul. Grunwaldzka 6, 60-780 Poznán, Poland.

0020-1693/86/$3.50

is also possible to observe the transitions arising from the energy-level splitting and selection-rule relaxation due to the nuclear electric quadrupole.

Experimental

Sample Preparation

The 1,1,1,5,5,5-hexafluoroacetylacetone (hfa) was obtained from Eastman Kodak Corporation and redistilled before use. Purity was checked by boiling point and NMR spectra. Reagent grade acetates of zinc, magnesium and manganese were used without further purification.

Syntheses of the chelates

To 25 ml of chloroform, 0.01 mol of the ligand was added. In a separate container 0.005 mol of the appropriate metal acetate was dissolved in 50 ml of boiling chloroform. This hot solution was added slowly to the boiling solution of hfa with stirring. The mixture was refluxed for 1 h. The products were purified by repeated recrystallization. The melting points of the chelates were: Mn, 160–1 °C; Zn, 165–6 °C; Mg, 187–8 °C.

Doped crystals of the *cis*-complex suitable for EPR investigation were prepared by dissolving 0.02 mol of Zn(hfa)$_2$ in boiling chloroform and adding about 1 mol-percent of the Mn(II) complex. It is necessary that the solution be saturated at 60 °C. Single crystals were obtained by slowly lowering the temperature of the solution. Single crystals of the pure host *cis*-Zn complex were prepared in the same manner Doped single crystals of the *trans*-chelate were grown by the slow evaporation, at room temperature, of saturated solutions of either the Zn or Mg chelate to which about 1 mol-percent of the Mn chelate had been added. Crystals of the Zn complex were grown from solutions to which no Mn chelate had been added.

X-Ray Data Collection and Reduction

(a) trans isomer

A plate-like crystal of the *trans* isomer was mounted on an Enraf-Nonius CAD-4 diffractometer; preliminary analysis demonstrated that the complex belongs to the orthorhombic system, the space group being either *Pnma* (No. 62) or *Pna*2$_1$ (No. 33); the former choice was confirmed by the structure refinement. Data collection parameters are assembled in Table I.

(b) cis isomer

Preliminary analysis suggested the monoclinic system, either *C*2/*c* (No. 15) or *Cc* (No. 9); the centrosymmetric choice was confirmed by the successful refinement. Parameters are collected in Table I.

TABLE I. Crystallographic and Data Collection Parameters

	trans	*cis*
a (Å)	7.430(5)	21 339(3)
b (Å)	21.965(8)	8.228(3)
c (Å)	11.096(4)	9.761(4)
β deg)		95.99(2)
V (Å^3)	1811(2)	1705(2)
Z	4	4
Space group	*Pnma* (No. 62)	*C*2/*c* (No 15)
NO($I > 3\sigma(I)$)	821	1170
Data range	$2 < 2\theta(\text{Mo}) < 48°$	$2 < 2\theta(\text{Mo}) < 50°$
μ (cm^{-1})	15.3	16.5
Maximum transmission (%)	99.98	99.88
Minimum transmission (%)	94.56	75.28
Average transmission (%)	97.80	90.90
R_1	0.057	0.041
R_w	0.055	0.041

Solution and Refinement of the Structures

Trans isomer

With four molecules in space group *Pnma* the zinc atoms must lie on an inversion center or on the mirror plane at $y = \frac{1}{4}$; the latter was confirmed and the *x*- and *z*-coordinates were obtained from a Patterson function, and the F, O, and C atoms were located in subsequent difference Fourier maps. The CF$_3$ group at C(1) exhibited some disorder. Isotropic refinement gave values of the conventional agreement factors $R_1 = \Sigma \| F_o | - | F_c \| / \Sigma | F_o |$ and $R_w = [\Sigma w(| F_o | - | F_c |)^2 / \Sigma w F_o{}^2]^{1/2}$ of 0.109 and 0.110, respectively. The hydrogen atoms associated with one bonded water molecule [OW(2)] and with ligand carbon atom C(3) were located and refined in subsequent iterations, but attempts to locate the hydrogen atoms associated with the unbound water [OW(3)] and the other bonded water [OW(1)] were not successful. Final refinement, involving isotropic refinement of the hydrogen atoms and anisotropic refinement of all other atoms, and using a 60/40 disorder model for the disordered CF$_3$ group, converged to values of $R_1 = 0.057$ and $R_2 = 0.055$; no parameter experienced a shift of more than 0.60^{-} in the final cycle. A difference Fourier map showed peaks of 0.22 e Å^{-3} in the vicinity of the CF$_3$ group at C(5), which may be indicative of some minor disorder at that site also but which could not be used to generate any meaningful disorder model. The refined positional parameters are collected in Table II.

cis isomer

With four molecules in space group *C*/2*c*, the zinc atoms are constrained to lie on either an inversion

TABLE II. Atomic Positional Parameters for *trans*-[Zn(hfa)$_2$(H$_2$O)$_2$]·H$_2$O

Atom	x	y	z
Zn	0.1920(2)	0.2500(0)	0.0398(1)
F5A	0.5443(10)	0.0422(3)	0.0997(6)
F5B	0.6712(9)	0.1253(3)	0.1149(8)
F5C	0.514(9)	0.0974(3)	0.2515(6)
F1A	0.0895(15)	0.0392(5)	−0.1778(8)
F1B	−0.0481(16)	0.1154(5)	−0.2330(10)
F1C	−0.1486(15)	0.0677(7)	−0.0885(10)
F1A1	−0.1875(23)	0.1175(8)	−0.1531(14)
F1B1	0.0351(24)	0.0970(11)	−0.2497(16)
F1C1	−0.0686(20)	0.0421(7)	−0.0916(16)
OW1	0.3640(11)	0.2500(0)	−0.1168(7)
OW2	0.0072(12)	0.2500(0)	0.1829(8)
OW3	0.2431(12)	0.2500(0)	0.6375(8)
O2	0.0457(8)	0.1819(3)	−0.0422(5)
O4	0.3502(8)	0.1846(2)	0.1187(5)
C2	0.101(1)	0.1295(4)	−0.0541(7)
C3	0.250(1)	0.1026(4)	−0.0013(7)
C4	0.360(1)	0.1315(4)	0.0813(7)
C1	−0.009(1)	0.0878(6)	−0.1366(9)
C5	0.515(1)	0.0949(5)	0.1350(10)
H3	0.288(9)	0.065(3)	−0.018(5)
HW2	−0.052(12)	0.212(3)	0.218(7)

center or the twofold axis; the latter was confirmed by examination of a Patterson function. Both CF$_3$ groups are disordered, that at C(1) exhibiting 90/10 disorder while that at C(5) is 85/15. The three independent hydrogen atoms, one on C(3) and two on OW, were located and refined isotropically, as were the minor contributors to the CF$_3$ disorder [atoms F(1)A′–F(5)C′], while other non-hydrogen atoms were refined anisotropically to give $R_1 = R_w = 0.041$. A final difference Fourier was featureless, with no peak higher than 0.14 e Å^{-3}. The refined positional parameters are assembled in Table III, see also 'Supplementary Material'. All computer programs were from the Enraf-Nonius CAD-4/SDP package.

Description of the Structures

(a) trans isomer

The structure consists of discrete monomeric [Zn(hfa)$_2$(OH$_2$)$_2$] units which are linked to each other and to the solvent water molecules by hydrogen bonds. A view of the complex is given in Fig. 1, and the hydrogen bonding and packing in the cell are depicted in Fig. 2. The principal bond lengths and angles in the complex are presented in Tables IV and V, respectively.

TABLE III. Atomic Positional Parameters for *cis*-[Zn(hfa)$_2$(H$_2$O)$_2$]

Atom	x	y	z
Zn	0.0000(0)	0.06890(9)	0.2500(0)
F1A	0.2054(2)	−0.0455(4)	0.1496(4)
F1B	0.1739(1)	0.1253(4)	−0.0018(3)
F1C	0.2387(1)	0.1997(5)	0.1645(3)
F5A	0.0839(2)	0.5459(4)	0.4955(4)
F5B	0.1713(2)	0.4314(5)	0.5559(4)
F5C	0.0902(2)	0.3497(5)	0.6386(3)
F1A′	0.2355(13)	0.072(3)	0.220(3)
F1B′	0.2121(15)	0.235(4)	0.093(3)
F1C′	0.1824(12)	0.027(3)	0.055(3)
F5A′	0.1326(10)	0.528(3)	0.484(2)
F5B′	0.0647(9)	0.435(2)	0.588(2)
F5C′	0.1448(11)	0.358(3)	0.614(2)
OW	−0.0317(1)	−0.1206(3)	0.1186(3)
O2	0.0836(1)	0.0776(3)	0.1621(2)
O4	0.0398(1)	0.2350(3)	0.3940(3)
C1	0.1892(2)	0.1078(6)	0.1324(5)
C2	0.1334(2)	0.1480(5)	0.2120(4)
C3	0.1428(2)	0.2478(5)	0.3238(4)
C4	0.0957(2)	0.2874(5)	0.4054(4)
C5	0.1100(2)	0.4071(6)	0.5235(5)
H3	0.185(2)	0.308(5)	0.342(3)
HW1	−0.059(4)	−0.104(10)	0.051(9)
HW2	−0.005(3)	−0.190(8)	0.080(6)

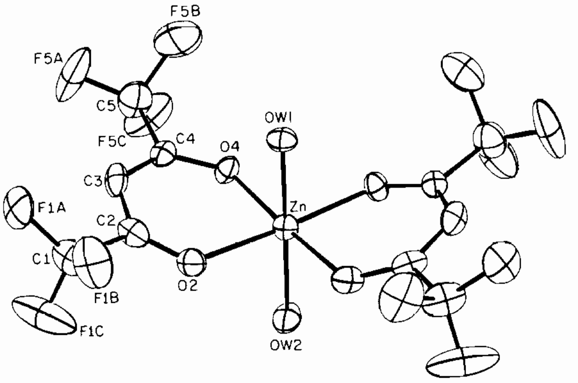

Fig. 1. View of the complex *trans*-[Zn(hfa)$_2$(OH$_2$)$_2$]. Thermal ellipsoids here and elsewhere drawn at the 30% probability level, and hydrogen atoms omitted for clarity.

The geometry at the zinc centers is constrained to be $C_s(m)$, the mirror plane passing through zinc and the two *trans* water molecules and relating one hfa ligand to the other. The angular distortions from idealized octahedral symmetry in this complex are very small, *trans* angles falling in the narrow range of 175.5(3) to 176.9(3)° while *cis* angles vary from 87.5(2) to 93.0(2)°. The Zn–O (ligand) bond lengths of 2.052(4) and 2.061(4) Å are similar to each other and are significantly shorter than the Zn–O (water) distances of 2.099(7) and 2.157(5) Å. The ligand geometry is normal, the partial double bonds C(2)–C(3) and C(3)–C(4) having similar bond lengths of 1.385(9) and 1.381(9) Å, respectively, while the nominally single C(1)–C(2) and C(4)–C(5) bonds are 1.532(11) and 1.529(10) Å, respectively; the C(2)–O(2) and C(4)–O(4) bond lengths of 1.213(8)

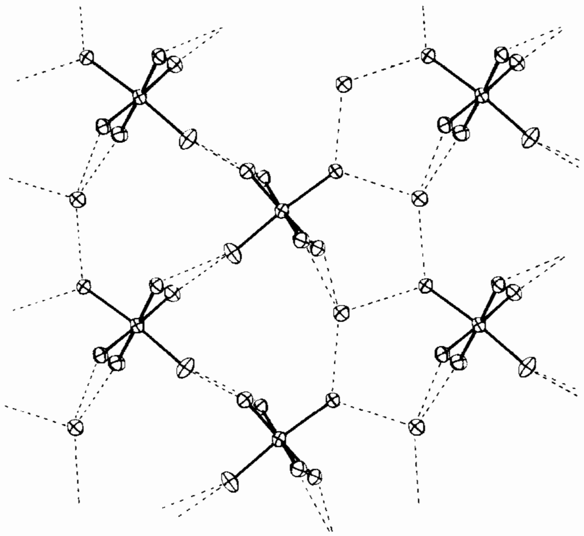

Fig. 2. The hydrogen bonding in *trans*-$[Zn(hfa)_2(OH_2)_2]\cdot H_2O$. The view is projected on the crystallographic *ac* plane, with *a* vertical and *c* horizontal.

TABLE IV. Bond Lengths (Å) in the *trans*- and *cis*-isomers of $[Zn(hfa)_2(OH_2)_2]$

Atoms	*trans*	*cis*
Zn–O(2)	2.061(4)	2.061(2)
Zn–O(4)	2.052(4)	2.077(2)
Zn–OW(1)	2.157(5)	2.086(2)
Zn–OW(2)[a]	2.099(7)	2.086(2)
C(1)–F(1)A[b]	1.374(17)	1.314(4)
C(1)–F(1)B	1.263(21)	1.324(4)
C(1)–F(1)C	1.246(21)	1.311(4)
C(1)–C(2)	1.532(11)	1.524(4)
C(2)–O(2)	1.231(8)	1.263(3)
C(2)–C(3)	1.385(9)	1.364(4)
C(3)–C(4)	1.381(9)	1.384(4)
C(4)–O(4)	1.240(6)	1.263(3)
C(4)–C(5)	1.529(10)	1.522(4)
C(5)–F(5)A	1.242(10)	1.287(5)
C(5)–F(5)B	1.357(9)	1.328(5)
C(5)–F(5)C	1.294(10)	1.327(5)

[a] In the *cis* isomer, these distances are equal by symmetry. [b] Only the distances to the principal component of disordered CF_3 groups are given here.

and 1.240(6) Å are also indicative of the aromatic character of the ligand. These distances are entirely comparable with those in other substituted acac complexes [7]. The chelate portion of the hfa ligands is planar, no atom deviating from the plane defined by O(2), C(2), C(3), C(4), O(4) by more than 0.012(9) Å; the zinc atom is significantly out of this plane, lying 0.417(1) Å above it while atoms C(1) and C(5) are slightly below it at distances of 0.084(10) and 0.028(11) Å, respectively. The chelate 'bite' distance is 2.88(1) Å leading to a chelate O(2)–Zn–O(4) angle of 89.0(2)°.

TABLE V. Selected Bond Angles (deg) in *trans*- and *cis*-$[Zn(hfa)_2(OH_2)_2]$

Atoms	*trans*	*cis*
O(2)–Zn–O(2)′	93.0(2)	176.00(11)
O(2)–Zn–O(4)	89.0(2)	87.05(7)
O(2)–Zn–O(4)′	176.9(3)	90.32(7)
O(2)–Zn–OW(1)[a]	87.5(2)	90.52(7)
O(2)–Zn–OW(2)[b]	89.4(2)	92.47(7)
O(4)–Zn–O(4)′	88.9(2)	97.73(11)
O(4)–Zn–OW(1)	90.3(2)	172.32(8)
O(4)–Zn–OW(2)	93.0(2)	89.56(7)
OW(1)–Zn–OW(2)	175.5(3)	83.27(10)
C(1)–C(2)–C(3)	115.2(9)	118.8(3)
C(1)–C(2)–O(2)	116.4(10)	112.0(3)
O(2)–C(2)–C(3)	128.4(7)	129.2(3)
C(2)–C(3)–C(4)	123.8(7)	123.2(3)
C(3)–C(4)–C(5)	117.5(7)	119.2(3)
C(3)–C(4)–O(4)	128.4(7)	127.2(3)
O(4)–C(4)–C(5)	114.0(7)	113.6(3)

[a] In the *cis* isomer, this is OW. [b] In the *cis* isomer, this is OW′.

As can be seen in Fig. 2, the hydrogen bonding in the crystals is extensive, with all potential donors and acceptors participating. Since we were unable to locate some of the water hydrogen atoms, a complete quantitative discussion of the hydrogen bonding is not justified. It is, however, apparent that the solvent water molecule OW(3) acts as a donor to atoms O(2) and O(4)′ of a given molecule, while acting as an acceptor from the bond water molecules OW(1) of two different complexes. The hydrogen bonding in the complex is summarized in tabular form in the supplementary material.

(b) cis isomer

The structure consists of monomeric $[Zn(hfa)_2(OH_2)_2]$ complexes which are linked by hydrogen bonds; a view of one complex is presented as Fig. 3,

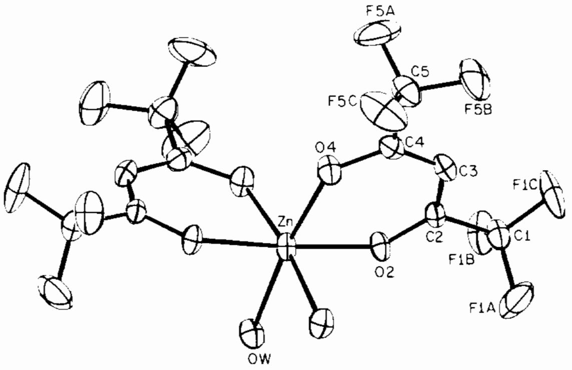

Fig. 3. View of the complex *cis*-$[Zn(hfa)_2(OH_2)_2]$.

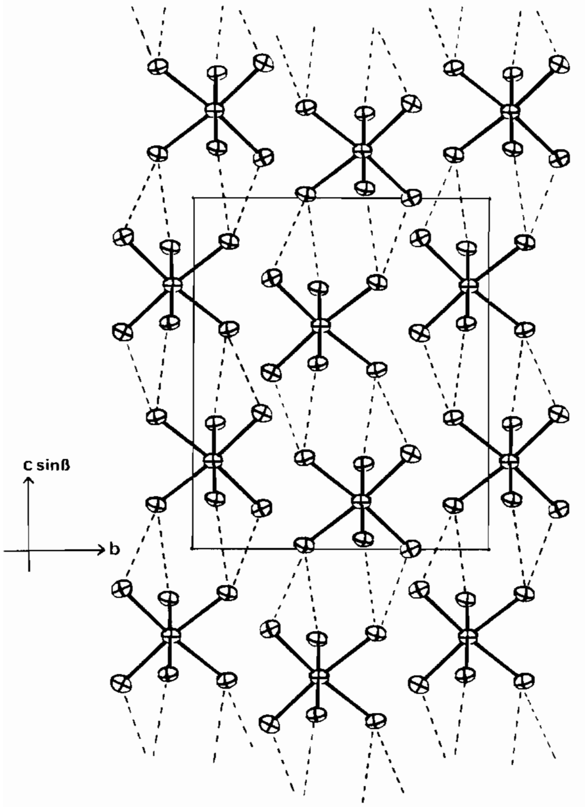

Fig. 4. The hydrogen bonding in *cis*-[Zn(hfa)$_2$(OH$_2$)$_2$]. The view is indicated on the figure.

and the hydrogen bonding is depicted in Fig. 4. The bond lengths and angles in this complex are compared with those in the *trans* isomer in Tables IV and V, respectively.

The geometry at the zinc atom is rigorously $C_2(2)$, the axis passing through the zinc atom alone and relating one ligand and one water molecule to the other. While the angular distortions from octahedral geometry are greater in this isomer than in the *trans* form, the six Zn–O distances fall in the narrow range of 2.061(2) to 2.086(2) Å; hence, in the *cis* isomer the water molecules appear to be more tightly bound than in the *trans* form. The ligand geometry is again unremarkable and similar to that found in the *trans* isomer and elsewhere [7]. The five-membered chelate moiety [O(2), C(2), C(3), C(4), O(4)] is approximately planar [maximum deviation 0.020(4) Å], but in this case the zinc is not as far out of the plane [0.151(1) Å] as in the *trans* isomer. The chelate 'bite' distance is 2.85 Å, the O(2)–Zn–O(4) angle being 87.05(7)°.

In the hydrogen bonding scheme, depicted in Fig. 4, each bonded water molecule OW acts as a donor to the O(2) and O(4)′ atoms of the same adjacent molecule, leading to the chain-like structure seen in the figure. The OW····O(2) and HW(1)····O(2) distances and OW–HW(1)····O(2) angle are 2.868(2), 2.10(1) Å and 151(1)° while the OW····O(4), HW(2)····O(4), and OW–HW(2)····O(4) parameters are 2.952(2) Å, 2.18(1) Å, and 143(1)°, respectively.

EPR Data Collection and Reduction

The EPR spectra were observed with a Varian E-9 spectrometer operating at X-band frequencies and a spectrometer constructed in the Clark Physics Department operating at K-band frequencies [6].

For the X-band measurements, the crystals were mounted on a quartz rod with a silicone optical coupling compound. A high power optical microscope was used to align each axis of rotation of the crystal parallel to the axis of the rod. The rod was attached to a Varian E 229 goniometer which allowed rotation of the crystal with respect to the applied magnetic field. Calibration of the applied field was accomplished with a Magnion Gaussmeter and the klystron frequency was measured with a Hewlett-Packard model 5246L frequency counter equipped with a 5255A frequency converter.

(a) trans isomer

Data collection followed the same techniques previously described [7]. The second derivative of the EPR absorption spectrum was recorded at 5° intervals in planes perpendicular to the axes labelled *a, b* and *c* in Fig. 5a. The nomenclature identifies

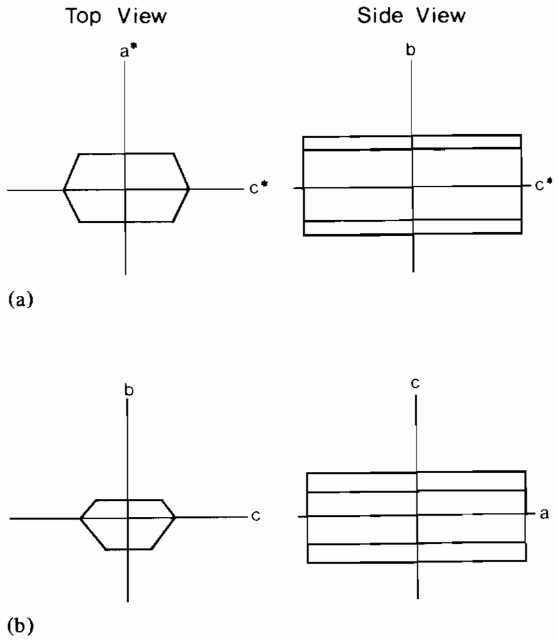

Fig. 5. Crystallographic axes with respect to the crystal morphology; (a) *cis* isomer, (b) *trans* isomer.

the appropriate crystallographic axis. The *trans* isomer was studied doped into single crystals of the Zn-chelate and single crystals of the Mg-chelate. The Mn-spectrum was essentially the same for both host crystals, a strong indication that the two host crystals are isomorphous. The spectra were characteristic of a tetragonally distorted octahedral geometry about the Mn(II) ion. Both host materials showed two magnetically inequivalent sites which gave rise to spectra that overlapped so badly that an analysis could not be carried out for the values of the spin-Hamiltonian parameters in two of the three principal directions. Fortunately in the *a*-direction the magnetic axes of the two sites are equivalent so that the spectrum could be observed along this principal magnetic direction. Along a principal magnetic axis the spectrum consists of five groups of six transitions arising from transitions between the levels of a sextet spin state whose levels have been split through coupling with the nuclear moment of a nucleus with $I = 5/2$. The selection rules are, $\Delta m_s = \pm 1$, $\Delta m_I = 0$. Typical spectra have been published in refs. 2 and 3.

Nuclei with $I > ½$ possess an electric quadrupole moment. This quadrupole couples with the gradient of the extranuclear electric field to further split the energy levels. This interaction affects the electron spin energy in the second order through a nuclear-electron magnetic coupling. In the absence of an applied magnetic field, the energy levels of the nuclear moment will be quantized along the z-component of the crystal field. If a magnetic field is applied parallel to the field axis, the only effect is a small displacement of all the energy levels by a constant amount which will have no effect on the observed transitions. However, when these two axes are not parallel, there is a competition between the electric field and the magnetic field to determine the axis of quantization. This has two effects on the spacing of the hyperfine lines: (1) a displacement of all energy levels by a constant amount and (2) a change in the separation of the energy levels such that the spacing of the hyperfine transitions is greater near the ends of a group than in the middle. The effects of the energy perturbations are generally much smaller than the effect of other terms in the spin-Hamiltonian. A more important consequence of this effect is the resulting relaxation of the $\Delta m_I = 0$ selection rule so that transitions corresponding to $\Delta m_I = \pm 1, \pm 2$ are observed. This nuclear quadrupolar effect has been seen in only two other Mn(II) chelates [2, 3].

The data were reduced by standard methods developed by Abragam and Pryce [8], Bleaney and Ingram [9] and Folen [10]. The effective spin-Hamiltonian derived by Abragam and Pryce and applied by Bleaney and Ingram is,

$$\mathcal{H} = g\beta H\cdot S + D\left\{S_z^2 - \frac{1}{3}S(S+1)\right\} + E(S_x^2 - S_y^2) + F(\mathrm{a}) + AS_z\cdot I_z + B(S_xI_x + S_yI_y) - \gamma\beta_N H\cdot I + Q\left\{I_z^2 - \frac{1}{3}I(I-1)\right\} \quad (1)$$

In this expression the symbols have their usual meaning. $F(\mathrm{a})$ represents the cubic portion of the crystal field and is given by,

$$\frac{\mathrm{a}}{6}(S_\xi^4 + S_\eta^4 + S_\zeta^4) - \frac{1}{5}S(S+1)[3S(S+1) - 1] \quad (2)$$

In the present cases the ξ, η, ζ axes coincide with the x, y, z axes. From Bleaney's Hamiltonian, Folen [10] arrived at the following equations for the transitions, complete to the second order in the spin-Hamiltonian parameters:

$$\begin{aligned}\mathcal{H} = {} & H_o - (2M_S - 1)\mathrm{D} - A_z m_I - \left(\frac{A^2}{2H}\right)[I(I+1) - m_I^2 + (2M_S - 1)m_I] \\ & + \left(\frac{A^2D}{2H^2}\right)\{3[I(I+1) - m_I^2](2M_S - 1) - m_I[2S(S+1) + 3(-2M_S^2 + 2M_S - 1)]\} \\ & - \left(\frac{A^3}{2H^2}\right)\{[2I(I+1) - 3m_I^2](2M_S - 1) + m_I[-S(S+1) - I(I+1) - 3M_S^2 - 3M_S + m_I^2 + 2]\} \\ & - \left(\frac{E^2}{2H}\right)[2S(S+1) - 6M_S^2 + 6M_S - 3] + \left(\frac{E^2D}{H^2}\right)\{2(M_S - 1)[3S(S+1) - 5M_S^2 + 5M_S - 6)]\} \\ & + \left(\frac{E^2Am_I}{2H^2}\right)[2S(\mathrm{S}+1) - 6M_S^2 + 6M_S - 3]\end{aligned} \quad (3)$$

The hyperfine constant, A, is considered isotropic for the higher order terms which turns out to be a valid approximation. Transitions for the applied field parallel to the y- and x-principal magnetic axes are obtained from the above relationship by replacing the quantities g_z, A_z, D and E by g_y or g_xA_y or A_x, $(D - 3E)/2$ or $(D + 3E)/2$ and $(D + E)/2$ or $(D - E)/2$, respectively.

Folen's equations provide a convenient starting point for the reduction of the data, for they relate directly to observables. Thus, the 30 transitions observed when H is parallel to the z-magnetic axis were fitted to these equations by the method of 'least squares' by use of a program which iteratively improves a set of initial estimates of the parameters until the change in each parameter is less than 1 part in 10^5 between two successive iterations. The experimental measurement and the values calculated from the final fitting equation agree to better than 1 part in 10^4 for all measurements. The values of D, A, and g are determined to better than 0.1%. However the value of E, since it is determined from higher order terms in the transition equation may not be any better than 20%. The parameters determined by this procedure are given in Table VI.

TABLE VI. Spin-Hamiltonian Parameters for the *trans* Isomer

	Mn(II) doped Zn(hfa)$_2$	Mn(II) doped Mg(hfa)$_2$
g_z	1.9960 ± 0.0003	1.9995 ± 0.0003
D (gauss)	401 ± 1.25	403 ± 1
E (gauss)	71 ± 5	70 ± 5
A_z (gauss)	91.8 ± 0.5	91.9 ± 0.4

The observation of the $\Delta m_I = \pm 1$, ± 2 transitions allows, in principle, the determination of the quadrupole interaction constants defined as, $Q' = 3eQq/4I(2I - 1)$ and $Q'' = 3eQq\eta/4I(2I - 1)$, where Q' is the axial part of the quadrupole interaction and Q'' is the rhomic part [10]. Their determination is most conveniently made from the $\Delta m_I = \pm 1$ transitions that appear as doublets between the $\Delta m_I = 0$ transitions in the $m_s = 1$ transition, $|½, m_I > | -½, m_I >$. The expression for the separation of these doublets as given by Folen [10] is,

$$\begin{aligned}\Delta H_d &= H(M_S = ½, m_I + 1 \longrightarrow M_S = -½, m_I) \\ &\quad - H(M_S = ½, m_I \longrightarrow M_S = -½, m_I + 1) \\ &= 17A^2/2H + (2g_N\beta_N/g\beta)H - \{Q' - 4A^2D/H^2) \\ &\quad \times (3\cos^2\theta - 1) + (3Q'' - 4A^2E/H^2) \\ &\quad \times \sin^2\theta \cos^2 \;+ 25A^3/2H^2\}(2m_I + 1), \qquad (4)\end{aligned}$$

It can be seen that the determination rests on the difference between successive pairs of doublets. In the *trans* isomer, Q'' is small so that the differences between successive doublets is likewise small, about 0.3 G, with a large error. Thus the value determined Q' = –0.5 G must be regarded as tentative.

(b) cis isomer

The *cis* isomer, observed in a host lattice of the Zn-chelate, exhibited only one magnetic site per unit cell. This allowed the observation and analysis of the EPR spectrum along each of the principal magnetic axes. Spectra were observed in the a^*c^* plane by rotating the crystal about the b-axis. Two of the principal magnetic axes were found in this plane, the first making an angle of about 65° with the c^* axis and the other 90° away at 155° from the c^*-axis. The third principal axis was found in the bc^*-plane and coincides with the b-axis. Once again nuclear quadrupole induced transitions were observed. Again, the data were reduced by use of Folen's equations. The results are summarized in Table VII for measurements at both X-band and K-band frequencies. The spin-Hamiltonian parameters are in agreement within experimental uncertainty. The value of Q' is very small in the complex so cannot be determined from our data.

TABLE VII. Spin-Hamiltonian Parameters for the *cis* Isomer Zn(Hfa)$_2$ Host

	X-band Data	K-band Data
g_x	2.0098 ± 0.0003	2.0092 ± 0.0003
g_y	2.0000 ± 0.0003	2.0007 ± 0.0003
g_z	2.0002 ± 0.0003	2.0007 ± 0.0003
D (gauss)	170.1 ± 0.2	171.0 ± 0.8
E (gauss)	9 ± 2	10 ± 2
A_x (gauss)	92.58 ± 0.20	92.87 ± 0.60
A_y (gauss)	92.61 ± 0.20	92.74 ± 0.30
A_z (gauss)	92.67 ± 0.07	92.37 ± 0.35

The crystal structure results together with the EPR results enable the location of the magnetic axes within the chelate. One of these is coincident with the twofold symmetry axis which bisects the H_2O–Zn–H_2O angle. The other two bisect the two chelate rings. This is consistent with the results found for transdiaquobis(acetylacetonato)Mn(II) [3]. In a large number of copper(II) complexes it has also been found that the magnetic axes generally bisect the chelate rings.

Discussion

The results of the EPR studies are consistent with results from previous EPR studies of Mn(II) chelates. For the *cis* compound, for which the spectra could be observed with the magnetic field parallel to each of the principal axes, it was found that the g- and A-

values are essentially isotropic. The spin-Hamiltonian parameters derived from the X-band observations and the K-band observations are in excellent agreement. The value of D is one of the lowest that has been observed for a Mn(II) chelate with octahedral coordination. Further, the very low value of E is consistent with the z-axis of the crystal field being coincident with the twofold molecular axis with the x- and y-axes bisecting the chelate rings. This is the first example of a *cis*-coordinated chelate of Mn(II) that has been studied by EPR, hence, there are no other results to compare with these.

The results for the *trans* isomer are somewhat less satisfying because of the presence of two magnetically inequivalent sites in the crystal. As a result, the spectrum along only one principal magnetic axis could be observed and analyzed. The spectrum of this isomer was observed in two different host lattices, that of the Zn(II)-chelate and that of the Mg(II)-chelate. The spectra that were observed in the two hosts could be essentially superimposed, a strong indication that the two host lattices are isomorphic. Further, the spin-Hamiltonian parameters determined in the two samples were in excellent agreement.

The results can be compared to those for the *trans*-diaquobis(acetylacetonato)Mn(II) doped into a host lattice of the Mg(II) chelate [$Mn(acac)_2$] [3]. $Mn(acac)_2$ is air and light sensitive. The crystals were grown from dimethylformamide under nitrogen and in the dark. *trans*-$Mn(hfa)_2$ is stable in air at room temperature and suitable crystals were grown from a covered beaker under normal conditions. The crystal structures of the two host lattices in the two studies are quite different. In the $Mn(acac)_2$ the *trans* oxygen molecules are symmetrically disposed while in the $Mn(hfa)_2$ the bond distances differ markedly. Also, there is an extra molecule of water in the $Mn(hfa)_2$ lattice.

Only one A-value could be observed for the fluorinated chelate and its value is very close to the average of the three observed A-values for $Mn(acac)_2$. There is more anisotropy in these three observed A-values than has been reported for any other Mn(II) chelate. The zero-field splitting $D = 702$ G in $Mn(acac)_2$ is much larger than that of 401 G observed for $Mn(hfa)_2$. Title [11, 12] has proposed a linear relationship between A-value and ionicity of the lattice with A decreasing with increased ionicity. One would expect metal–ligand bonds to be more ionic in the fluorinated chelate, but no effect on A is observed. The sizeable difference in D-values may well arise from a smaller ligand field in $Mn(hfa)_2$, or because the only observed value is not along the principal axis of greatest D. There is no ligand-field stabilization for high spin d^5 ions so its strength cannot be measured by normal methods. However, there is evidence that for strongly electronegative ligands with filled p-orbitals on the bonding atom of the ligand, the ligand field is reduced [13]. Although this study does not provide the mechanism leading to an observable value of D in d^5 systems, it does shed some light on the problem and constitutes an advance toward the eventual quantitative solution.

Supplementary Material

Tables of anisotropic thermal parameters and listings of observed and calculated structure amplitudes for both molecules are available as supplementary material.

References

1 B. R. McGarvey, *Transition Met. Chem.*, *3*, 89 (1966).
2 H. J. Stoller, G. Rist and Hs. H. Gunthard, *J. Chem. Phys.*, *75*, 4651 (1972).
3 C. J. O'Connor and R. L. Carlin, *Inorg. Chem.*, *14*, 291 (1975).
4 D. J. E. Ingram, *Phys. Rev.*, *90*, 711 (1953).
5 D. J. E. Ingram, *Proc. Phys. Soc. London, Ser. A*, *66*, 412 (1953).
6 D. Close, *Thesis*, Clark University, 1973.
7 R. L. Lancione, H. C. Allen, Jr. and D. R. Sydor, *J. Coord. Chem.*, *4*, 153 (1975).
8 A. Abragam and M. H. L. Pryce, *Proc. R. Soc. London, Ser. A*, *205*, 135 (1951).
9 B. Bleaney and D. J. E. Ingram, *Proc. R. Soc. London, Ser. A*, *205*, 336 (1951).
10 V. J. Folen, *Phys. Rev.*, *131*, 1581 (1962).
11 R. S. Title, *Phys. Rev.*, *131*, 623 (1963).
12 R. S. Title, *Phys. Rev.*, *130*, 17 (1963).
13 J. E. Huheey, 'Inorganic Chemistry', 2nd edn., Harper and Row, New York, 1978, p. 401.